JOURNAL OF OPTOELECTRONICS AND ADVANCED MATERIALS Vol. 11, No. 10, October 2009, p. 1384 - 1387

A simulation study and theoretical Raman spectra of cryolitic melts

S. UCAR*, S. CIKIT, Z. AKDENIZ
Istanbul University, Physics Department, 34459 Vezneciler, Istanbul-Turkey

In order to study the nature of the liquid phase numerically, we need a computer simulation method which will yield the dynamical properties of the liquid. In this work, the method of Madden et al. (Castiglione, M.; Wilson, M., Madden, P.A. Phys. Chem. Phys. 1999, 1, 165.) was used within a molecular dynamics calculation to obtain the structural properties of liquid Na_3AlF_6 (Cryolite). In this system, the Al-Al, Al-Na, Al-F and Na-F radial distribution functions and the coordination numbers of the Al^{3+} ion are obtained near or above the melting point. We also determined that the systems which are not crystallized are in the liquid phase, by analyzing the diffusion coefficients with temperature changes. The theoretical Raman spectra of the system of interest were calculated by computer simulation and the effect of temperature on the results were examined in detail. The relationship between the bands appearing in the spectra and the vibrational modes of the AlF_6, AlF_5 and AlF_4 complex ions, which are present in these melts is discussed, in order to see how the Raman spectra reflect the coordination structure around the Al^{3+} ions.

(Received November 5, 2008; accepted December 15, 2008)

Keywords: Cryolitic melts, Raman spectra, Computer simulation

1. Introduction

Melts of the general composition MX_3/AX (where M is a trivalent metal, X a halogen, and A an alkali) are of interest in a number of electrochemical technologies [1,2]. Molten cryolite (Na_3AlF_6) is a liquid of tremendous economic importance, since it is the liquid in which aluminium oxide is dissolved in the electrolytic extraction of aluminium (the Hall-Herault process [1]) and is also used as a "solvent" in the extraction of other refractory metals, such as Nb. The coordination chemistry of the aluminium ions in liquid cryolite determines, in part, the efficiency of the extraction. It is controlled, in the industrial processes, by the addition of other substances. Despite its significance, there are no neutron or X-ray diffraction data to allow a direct determination of the coordination environment of the Al^{3+} ions, due to the high melting temperature and consequent difficulties of sample containment.

In recent papers [3,4], it has been shown that it is possible to simulate the Raman spectra of moderately complex molten salts. A model for the fluctuating polarizability of the melt on the ionic positions, which had been suggested by electronic structure calculations [5,6], was combined with a polarisable interaction potential [7], refined on the basis of structural studies. The simulations offer a way of bridging an interpretative gap between the structure as seen spectroscopically, where attention focuses on the coordination complexes responsible for the discrete Raman bands, as in a molecular system, and in diffraction experiments, where the data is discussed from a more atomistic perspective in terms of radial correlations in an ionic mixture [8,9]. Recently, the character of the ion dynamics in crystalline cryolite, Na_3AlF_6, a model double perovskite-structured mineral, has been examined in computer simulations using a polarizable ionic potential obtained by force-fitting to ab initio electronic structure calculations.

In this work, the interaction potential consists of a pair potential of Born-Mayer form, that is considered from the ab initio `force-fitting` potential parameters obtained in crystal cryolite [10]. The dispersion coefficients and dispersion damping parameters in the simulation potential are taken from [11].

2. Expression for the Raman spectra

The theory of the calculation of the Raman spectrum was discussed at length in [3]. The light scattering spectrum [11,12] for the scattering geometry characterized by the scattering vector q, where the polarizations of the incident and scattered radiation are the Cartesian directions b and a is proportional to the spectrum of the correlation function of the q^{th} spatial Fourier component of the polarizability density of the system, Π_{ab}, that is

$$I_{ab}(q,\omega) \mu \, Re\int_0^\infty dt \, e^{i\omega t} \left\langle \Pi_{ab}(q,t) \, \Pi_{ab}(q,0)^* \right\rangle \qquad (1)$$

For an ionic material, we [5,6] distinguish four contributions to the polarizability:

$$\Pi_{ab} = \Pi_{ab}^{SR} + \Pi_{ab}^{\gamma} + \Pi_{ab}^{B} + \Pi_{ab}^{DID} \qquad (2)$$

The terms Π_{ab} and Π_{ab}^{γ} represent the changes in the

anion polarizability by hyperpolarization via the interionic Coulomb field, where B and γ are the dipole- quadrupole and dipole-dipole- dipole hyperpolarizabilities of the ion [13]. Π_{ab}^{DID} is the contribution due to first-order dipole-induced dipole effects, and Π_{ab}^{SR} is that due to the changes in the polarizability α_{ab}^{i} of an anion by the compression and deformation of the ion by its short-range interactions with its neighbours [6]. Detailed expressions for these different polarizability mechanisms, in terms of the ionic coordinates, are given in [3, 5, 6], as well as values for the implicit parameters used in the present simulations.

The light scattering spectrum of an ionic system is thus quite complicated, as four mechanisms, with different dependencies on the interionic separations, can be expected to contribute. As discussed in the Introduction, the primary interest is in the isotropic spectrum, which reflects fluctuations in the trace of the polarizability density

$$\Pi_I = \Pi_{xx} + \Pi_{yy} + \Pi_{zz} \tag{3}$$

and dominates the polarized spectra. It can be shown that only the short-range (Π^{SR}) and gamma (Π^{γ}) mechanisms contribute to the trace of Π, due to the traceless nature of the dipole-dipole interaction tensor and the Coulomb field gradient. The isotropic spectrum can thus be regarded as the sum of three terms, the spectra of the autocorrelation functions of Π_l^{SR} and Π_l^{γ}, which we call the SR and γ "subspectra", plus the spectrum of their cross-correlation function.

2.1 Interaction potential

The interaction potential consists of a pair potential of Born-Mayer form, taking into account the interaction polarization [14]. The pair potential is written as

$$V(r_{ij}) = B^{ij} e^{-\alpha^{ij} r_{ij}} - f_{ij}^{6}(r_{ij}) \frac{C_{ij}^{6}}{r_{ij}^{6}} - f_{ij}^{8}(r_{ij}) \frac{C_{ij}^{8}}{r_{ij}^{8}} \tag{4}$$

where C_{ij} are the dispersion coefficients and F_{ij} are dispersion damping functions given by

$$f_{ij}^{n}(r_{ij}) = 1 - e^{-\left(b_{ij} r_{ij}\right)} \sum_{k=0}^{n} \frac{\left(b_{ij} r_{ij}\right)^{k}}{k!} \tag{5}$$

Values for all parameters are given in Table 1. The polarization parts of the potential include the fluoride ion polarization only [7,14]. We used a fluoride ion polarizability of 6.88 a.u., and applied a damping function

$$g_{ij}(r_{ij}) = 1 - c_{ij} e^{-\left(b_{ij} r_{ij}\right)} \sum_{k=0}^{4} \frac{\left(b_{ij} r_{ij}\right)^{k}}{k!} \tag{6}$$

to the interaction between the anion dipoles and the cation charges with $b_{FAl} = 1.8\ a.u^{-1}$, $b_{FNa} = 1.8\ a.u^{-1}$, $c_{FAl} = 1.5\ a.u^{-1}$, $c_{FNa} = 1.5\ a.u^{-1}$.

2.2 Details of the simulations

The simulations were carried out with polarizable ion interaction potentials as described in [15]. The potential given above has now been used in simulations of the melts over the range of the composition Na_3AlF_6. We decided to simulate our systems at the zero pressure. Before beginning this, we made small adjustments to the interaction potentials, so that the pure melts ($AlF_3$and NaF) had the correct molar volume [16] at 1250 K and zero pressure, and the mixtures were close to the experimental densities [17]. The new potential parameters are given in Table 1.

Only the F^- and Na^+ ions were treated as being polarizable; the polarizability of Al^{3+} is tiny. The calculations were carried out at temperatures close to the melting point, 1250 K. We followed the same protocol for all simulations. All of the runs contained 360 ions, depending on the stoichiometry. We carried out a 100,000 step equilibration run (36 ps) in an NPT ensemble, using the integration algorithm suggested by Martyna et al.; [18]. In all cases, the system settled to a density close to the experimental one [17] (typically about 2% larger). We then performed a 500,000 step NVT run, for the cell volume to which the system had equilibrated at zero external pressure, during which time correlation functions, and so forth, were calculated. Ewald sums were used for all Coulomb and multipolar interactions [19].

Table 1. Pair potential parameters[a]

Ion pair	B_{ij}	α_{ij}	C_{ij}^6	C_{ij}^8	b_{ij}^6	b_{ij}^8
F^- - F^-	120.93	2.20	63.337	777.897	1.6	1.6
Al^{+3}- F^-	111.43	2.35	0.0	0.0	2.9	2.9
Na^+-F^-	73.79	2.10	12.061	45.0	1.9	1.9
Al^{+3}-Al^{+3}	93.26	2.91	0.0	0.0	1.5	1.0
Na^+-Na^+	163.76	4.73	1.588	0.0	2.9	2.9
Al^{3+}-Na^+	0.0	0.0	0.0	0.0	1.5	1.0

[a] All of the parameters are given in atomic units.

3. Simulated Raman spectra of Na_3AlF_6

In Fig. 1, we show a snapshot of the ionic positions taken from the simulation at the cryolite composition (Na_3AlF_6) and at 1250 K. Lines indicate "bonds" between Al and F ions, if they are separated by less than the first minimum in the radial distribution function. The snapshot indicates that at this composition the melt contains four-, five-, and six-fold coordinated Al species. In this section, we will examine how they contribute to the features observed in the Raman spectrum.

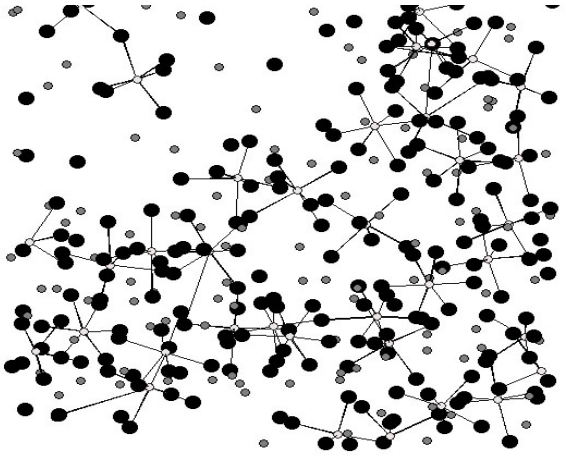

Fig. 1. Snapshot of the ionic positions in a simulation of the Cryolite composition (Na_3AlF_6). The F^- ions are shown in black, the Al^{3+} in white, and the Na^+ in gray.

3.1 Isotropic SR spectrum

We begin by describing the isotropic spectra calculated from the MD runs at 1250 K. In Fig. 2, it can be seen that the peaks in the densities of states shift to lower frequencies in the sequence AlF4 - > AlF5 2- > AlF6 3- and that, furthermore, there is a good correspondence between the density of states (DoS) peaks in the figure and the features seen in the Raman bands shown in Fig. 3. Contrary to the expectation from previous simulation results [11], we found that the SR spectrum has a different shape from the γ one, as we see in the top panel of Fig. 3. In particular, it is tempting to say, from the correspondence of the band positions with the peaks in the DoS, that the SR Raman band for Na_3AlF_6 is dominated by the six-fold coordinated complex. In Fig. 3, we also report the effect of temperature changes on the Raman spectrum in the simulations.

3.2 Isotropic γ spectrum

We show the subspectra associated with the γ polarizability mechanism in the bottom panel of fig. 3. We illustrate the relationship between the isotropic γ Raman subspectra and the DoS of the normal modes for the 4- , 5- and 6- fold coordinated species present in the cryolite melt.

Table 2 shows that the vibrational frequencies of the symmetric stretching vibrations extracted from our simulations, denoted PM, are in surprisingly good accord with those extracted from the experiments given in [11].

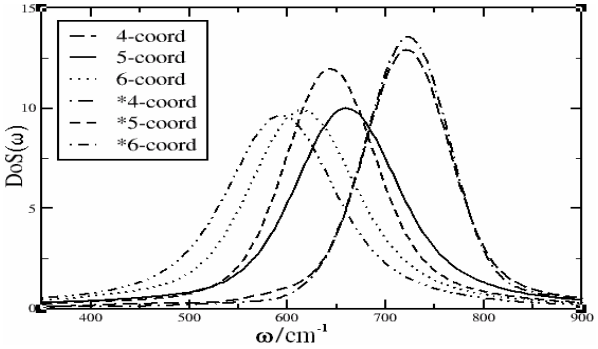

Fig. 2. The DoS of the symmetric breathing vibrations of four, five and six-fold coordinated complexes, calculated with our potential.

***** the values calculated with the force-fitting potential [10].

Table 2. Peak Frequencies of the symmetric stretching DoS spectra at 1250 K in AlF_3/3NaF mixtures[a]

AlF_3/3NaF	6-coord.	5-coord.	4-coord.
Experiment[11]	594	643	723
Na_3AlF_6 [11]	545	579	628
Na_3AlF_6 PM	615	658	723

[a] Symmetric stretching modes [cm^{-1}]

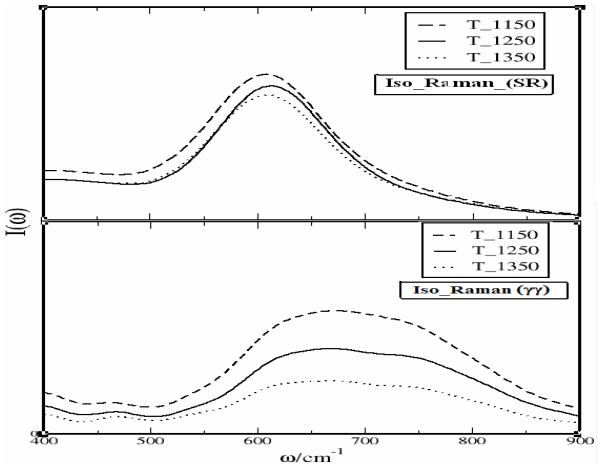

Fig. 3. Temperature dependence of the calculated isotropic Raman spectra for the cryolite composition, for the short-range and γ mechanisms.

In Fig. 4, we show mean square displacements (MSD) of the ionic species. One can find the diffusion coefficients via the slopes of the lines. We have confirmed that the system has not crystalized and is still liquid-like, by checking the diffusion coefficients by decreasing the temperatures.

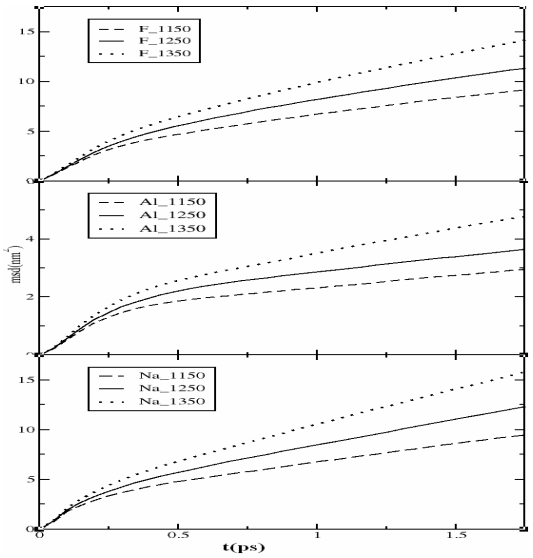

Fig. 4. The MSDs of the ions as a function of time, for cryolite.

4. Discussion

We have described calculations of the isotropic Raman spectra of cryolite, and have obtained spectra that are similar to those obtained experimentally. The isotropic gamma spectra show a quite good correspondence between the DoS peaks of the symmetric breathing vibrations, which suggests that the Al-F interactions have been described well by our interaction potentials.

Our spectral results provide a good description of the coordination clusters containing four, five and six fold-coordinated ions, as invoked in the explanation of the experimental data on cryolite [11].

Acknowledgments

One of us (S.C.) acknowledges support from the Research Foundation of Istanbul University, under Project Number T-826. (Z.A.) acknowledges support from TUBITAK.

References

[1] K. Grjotheim, Aluminium Electrolysis, Aluminium-Verlag, Düsseldorf, 1982.
[2] H. Matsuura, R. Takagi, M. Zbalocka-Malicka, Nucl. Sci. Technol. **33**, 895 (1997).
[3] P. A. Madden, M. Wilson, F. Hutchinson, J. Chem. Phys. **120**, 6609 (2004).
[4] W. J. Glover, P. A. Madden, J. Chem. Phys. **121**, 7293 (2004)
[5] P. A. Madden, J. Board, K. O'Sullivan, P. W. Fowler, J. Chem. Phys. **94**, 918 (1991).
[6] P. A. Madden, J. Board, J. Chem. Soc., Faraday Trans. 2, **83**, 1891 (1987).
[7] F. Hutchinson, M. Wilson, P. A. Madden, Mol. Phys. **99**, 811 (2001).
[8] M. P. Tosi, D. L. Price, M. L. Saboungi, Annu. Rev. Phys. Chem. **44**, 173 (1993).
[9] M. Rovere, M. P. Tosi, Rep. Prog. Phys. **49**, 1001 (1986).
[10] F. Lindsay, P. A. Madden, J. Phys. Chem. B **110**, 15302 (2006).
[11] Z. Akdeniz, P. A. Madden, J. Phys. Chem. B **110,** 6683 (2006).
[12] B. J. Berne, R. Pecora, Dynamic Light Scattering, Wiley, New York (1976).
[13] A. D. Buckingham, Adv. Chem. Phys. **12**, 107 (1967).
[14] P. A. Madden, M. Wilson, Chem. Soc. Rev. **25**, 339 (1996).
[15] M. Castiglione, M. Wilson, P. A. Madden, Phys. Chem. Chem. Phys. **1**, 165 (1999).
[16] G. J. Janz, R. P. Tomkins, J. Phys. Chem. Ref. Data **12**, 659 (1983).
[17] T. Ostvold, R. Fernandez, Acta Chem. Scand. **43**, 151 (1989).
[18] G. J. Martyna, D. J. Tobias, Klein, M. L., J. Chem. Phys. **5**, 101 (1994).
[19] A. Aguado, P. A. Madden, J. Chem. Phys. **119**, 7471 (2003).

*Corresponding author: seviucar@istanbul.edu.tr